JOURNAL OF CATALYSIS 145, 159–165 (1994)

Polarized Total-Reflection Fluorescence EXAFS Study of Anisotropic Structure Analysis for Co Oxides on α-Al_2O_3 (0001) as Model Surfaces for Active Oxidation Catalysts

Masayuki Shirai, Tomoya Inoue, Hiroshi Onishi, Kiyotaka Asakura, and Yasuhiro Iwasawa[1]

Department of Chemistry, Graduate School of Science, The University of Tokyo, Hongo, Bunkyo-Ku, Tokyo 113, Japan

Received March 15, 1993; revised July 28, 1993

An *in situ* Polarized Total-Reflection Fluorescence Extended X-ray Absorption Fine Structure (PTRF-EXAFS) technique was developed to analyze anisotropic structures of metal sites on surfaces. The PTRF-EXAFS can provide structural information in two different directions, separately, parallel (*s*-polarization) and normal (*p*-polarization) to the support surface. This technique was used to analyze the anisotropic structures of two kinds of Co-oxides on α-Al_2O_3 (0001) which were derived from $Co_2(CO)_8$ and α-Al_2O_3 (0001). The Co-oxides on α-Al_2O_3 (0001) are regarded as model surfaces of Co-oxide catalysts supported on α-Al_2O_3 active for CO oxidation. The *s*- and *p*-polarized EXAFS analysis revealed that after contact of $Co_2(CO)_8$ with α-Al_2O_3 (0001), followed by oxidation with O_2 at 300 K, Co atoms occupied the threefold hollow sites of α-Al_2O_3 (0001) as monomers (Co–O = 0.208 nm). By oxidation at 873 K, the Co monomers aggregated to form small spinel-like particles $[Co_3O_4]_n$ with ca. 0.9 nm dimension. The anisotropic structure analysis shows that the particles of seven layers grew with the spinel (001) plane parallel to the α-Al_2O_3 (0001) plane.

INTRODUCTION

Structures of metal sites at support surfaces on which catalytic reactions proceed may be anisotropic, and they may also change anisotropically under vacuum, H_2, O_2, or catalytic reaction conditions. The Mo dimer catalyst is a typical sample which shows an anisotropic change of 0.04 nm in a lateral direction (Mo–Mo separation) and 0.01 nm in a longitudinal direction (Mo–SiO_2 separation) during ethanol oxidation (1). We need detailed information on the structures of active sites in at least two different directions and their changes during treatments of catalyst and reaction conditions to investigate the genesis of solid catalysis, catalytic reaction mechanisms, and to develop new selective catalytic systems (1, 2).

Extended X-ray Absorption Fine Structure (EXAFS) is a powerful technique that provides structural information nondestructively on metal or metal oxide phases highly dispersed on inorganic supports under reaction conditions (3). In the case of powder samples such as typical heterogeneous catalysts, the structures determined by EXAFS are averaged structures in every direction of a sample. When single crystals are employed as supports, however, characterization of metal sites on them can be achieved separately in two different bond directions parallel and normal to the surface by polarized X-rays stemming from synchrotron radiation. For *K*-edge EXAFS spectra of oriented samples, effective coordination numbers N^* are given by

$$N^* = 3 \Sigma \cos^2 \theta_i, \qquad [1]$$

where θ_i is the angle between the electric-field vector of the incident X-ray and the bond vector r_i (4). Thus, when the polarization of the incident X-ray is normal to the surface (*p*-polarization), the X-ray absorber's neighbors which lie along lines parallel to the surface do not contribute to EXAFS signals. These bonds are observable when *s*-polarized X-rays parallel to the surface are used. In reverse, the bonds normal to the surface are detectable by *p*-polarized EXAFS.

Also, for single crystal surfaces, we can get EXAFS signals from the surface phase in total-reflection conditions because the penetration depth of X-rays is small (<3 nm). Furthermore, the EXAFS signals with a high S/B ratio and under *in situ* conditions can be taken by a fluorescence EXAFS technique. By changing the orientation of the sample to polarized synchrotron radiation and using the total-reflection fluorescence method (PTRF-EXAFS), it is possible to determine the anisotropic structures on surfaces (5–12).

In this paper, we report the anisotropic structure analysis for Co-oxides on an α-Al_2O_3 (0001) single crystal surface as model structures of Co-oxides on α-Al_2O_3 catalysts which exhibit high activities for CO oxidation.

[1] To whom correspondence should be addressed.

0021-9517/94 $5.00

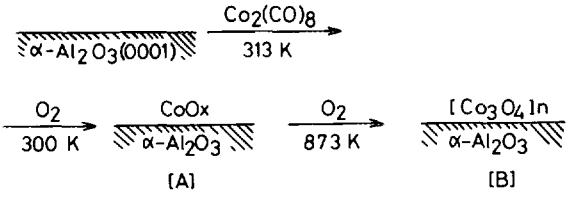

FIG. 1. Sample preparation steps.

2. EXPERIMENTAL

2.1. Sample Preparation

The samples were prepared as follows (Fig. 1). $Co_2(CO)_8$ (Strem Chemicals) was deposited on α-Al_2O_3 (0001) (Kyocera Inc., 10 × 30 × 1 mm^3) for 2 h at room temperature by a vapor deposition technique, followed by evacuation at 313 K under vacuum to remove excess Co carbonyls. Then the sample was exposed to O_2 (17 kPa) at 300 K for 5 h (sample [A]). The sample [A] was further oxidized in air at 873 K for 1 h to form the spinel-like sample [B].

$Co_2(CO)_8$ was also deposited on α-Al_2O_8 powder (Nishio Type 8000, surface area 20 m^2/g) in a similar way (13–16). The Co loading was 0.57 wt%.

The impregnated catalyst (0.68 wt%) was obtained by an impregnation method using an aqueous solution of $Co(NO_3)_2$, followed by drying at 393 K for 2 h and calcination at 773 K for 2 h in air.

2.2. XPS Measurement

The atomic ratio of Co atoms to surface oxygen atoms on α-Al_2O_3 (0001) was estimated by XPS (VG ESCA LAB-5) using reference samples ($Co(NO_3)_2 \cdot 6H_2O$/α-quartz(0001)) with a known amount of Co atoms.

2.3. CO Oxidation Reaction

CO oxidation reactions were carried out in a closed circulating system at 273 K and at a ratio of O_2 : CO = 6.6 : 3.3 (kPa).

2.4. PTRF-EXAFS Study

PTRF-EXAFS spectra were measured by BL-14A of the Photon Factory using a Si(111) double-crystal monochrometer in the National Laboratory for High Energy Physics (KEK-PF) as shown in Fig. 2 (Proposal No. 89-146). The storage ring was operated at 2.5 Gev with 350–200 mA. The Co *K*-edge EXAFS spectra were taken from 7430 to 8410 eV at the interval of 2 eV at 293 K. In order to set the sample at a particular orientation and to satisfy the total-reflection condition, a four-axis goniometer equipped at BL-14A (17) was used. The beam size was 0.1 mmϕ, which prevented unnecessary irradiation to other parts than the sample. The angle (θ_i) between the crystal face and the polarization was at 90° (*p*-polarization) and 0° (*s*-polarization). The incident X-ray was monitored by an ion chamber filled with N_2. Iron foil (thickness 0.01 mm) was used as a filter to minimize elastic scattering from the sample. A NaI scintillation counter was used to monitor the fluorescence EXAFS and its position was adjusted to remove the Bragg diffraction of X rays from the substrate.

The EXAFS spectra were extracted using a cubic spline method and normalized to the edge height. The κ^3-weighted EXAFS spectra were Fourier transformed to *r* space, and the inversely Fourier-filtrated data were analyzed using a curve fitting method on the basis of the single-scattering plane-wave theory (18), expressed by

$$\kappa^3\chi(\kappa) = N^* A(\kappa) \sin[2\kappa r_i + \phi_i]$$
$$A(\kappa) = F_i(\kappa) \exp(-2\sigma_i{}^2\kappa^2) \exp(-2r_i/\lambda_i(\kappa)) \quad [2]$$
$$N^* = 3\Sigma \cos^2\theta_i,$$

where κ is the wave vector of the photoelectron, and N_i^*, σ_i, r_i, and λ_i represent the effective coordination number of the *i*th shell, the Debye–Waller factor, and the interatomic distance of the *i*th shell, and the mean free path of the photoelectron, respectively.

The empirical phase shift ($\phi_i(\kappa)$) and amplitude function ($F_i(\kappa)\exp(-2r_i/\lambda(\kappa))$) obtained from the analysis of bulk Co_3O_4 were used for the analysis of Co–O and Co–Co (16).

Figure 3 shows the Fourier transform of transmission EXAFS data for Co_3O_4 powder in the κ-range from 30 to 130 nm^{-1}. There exist two Co sites in Co_3O_4 spinel, octahedral sites (Co(oct)) and tetrahedral sites (Co(tetra)). The first peak in the Fourier transform is assigned to Co–O, the second one to Co(oct)–Co(oct), the third one to Co(tetra)–Co(oct) and Co(tetra)–Co(tetra), and the fourth one to Co(oct)–Co(oct) behind the nearest neighbor Co(oct) (19). Averaged bond distances and coordination numbers for the EXAFS analysis are shown in Table 1.

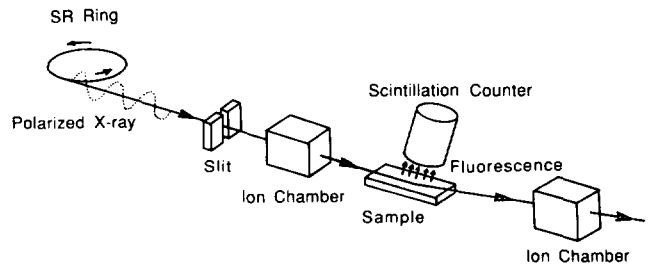

FIG. 2. A schematic diagram of polarized total-reflection fluorescence EXAFS.

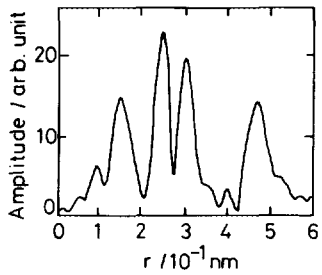

FIG. 3. The Fourier transform of transmission EXAFS for bulk Co_3O_4 powder.

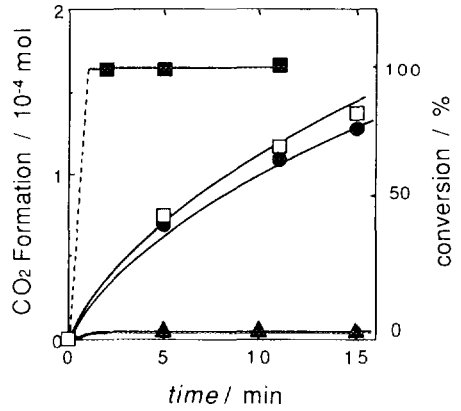

FIG. 4. CO oxidation on cobalt oxides on α-Al_2O_3 at 273 K: (■) sample [B], (□) sample [A], (●) impregnated catalyst, (▲) Pt/Al_2O_3 (reduced with H_2 at 573 K). CO: O_2 = 6.6:3.3 kPa. Catalyst weight: sample [A] and sample [B], 0.79 g (Co = 0.57 wt%); impregnated catalyst, 0.66 g (Co = 0.68 wt%); and Pt/Al_2O_3, 0.75 g (Pt = 1.7 wt%).

3. RESULTS AND DISCUSSION

It has been reported that small $[Co_3O_4]_n$ particles on SiO_2 and Al_2O_3 are remarkably active for CO oxidation (14, 16). The CO oxidation was suggested to proceed by a redox mechanism, as follows (14):

$$[Co_3O_4]_n + CO \rightarrow [Co_3O_{4-x}]_n + CO_2 \quad [3]$$

$$[Co_3O_{4-x}]_n + \tfrac{1}{2}O_2 \rightarrow [Co_3O_4]_n. \quad [4]$$

It was found that the 873 K-treated Co-oxides on α-Al_2O_3 (0001) (sample [B]) showed an extremely high activity for CO oxidation at 273 K as compared to the usual impregnation Co_3O_4 catalyst, as shown in Fig. 4. The catalytic activity of the sample [B] was so high that we could not follow the reaction rate. The 300 K-treated Co-oxides on α-Al_2O_3 (0001) (sample [A]) showed similar activity to that of the impregnation catalyst. As mentioned in the Introduction, PTRF-EXAFS can determine the structure of active Co sites more clearly than transmission EXAFS. The location of Co atoms on α-Al_2O_3 (0001) in the sample [A] and the asymmetric growth of spinel-like Co-oxides on α-Al_2O_3 (0001) in the sample [B] are described as follows.

3.1. Location of Co Atoms on α-Al_2O_3 (0001) Surface (Sample [A])

The Fourier transforms of *s*- and *p*-polarized EXAFS spectra for the sample [A] are shown in Fig. 5a and b, respectively, the κ-range for the Fourier transform was from 30 to 130 nm^{-1}. Only one peak between 0.1 and 0.2 nm is observed in both spectra, which is straightforwardly assignable to the Co–O bond, judging from the distance. There was no peak assigned to the Co–Co or Co–Al bond. This means that Co atoms exist as monomers on α-Al_2O_3 (0001). The curve-fitting analysis confirmed that the peak is due to the Co–O bond, and its bond distance was 0.208 nm in both polarizations (Table 2). The effective coordination numbers (N^*) of Co–O for *s*- and *p*-polarization were determined to be 3.3 and 3.9, respectively. The ratio of the two effective coordination numbers ($N^*(p)/N^*(s)$) is 1.2 (Table 2).

The arrangement of surface oxygen atoms at α-Al_2O_3 (0001) surface is hexagonal (19). There are three typical location sites of Co atoms on the α-Al_2O_3 (0001): "on-top," "bridge," and "three-fold hollow" sites. Moreover, considering the Al atoms which exist in the second layer, the possible Co sites are discriminated into one "on-top" site (O_1), two kinds of "bridge" sites (B_1 and B_2), and three kinds of "threefold hollow" sites (T_1, T_2, and T_3) as shown in Fig. 6.

TABLE 1

Averaged Bond Distances and Coordination Numbers Calculated from X-Ray Crystallographic Data of Co_3O_4 for EXAFS Analysis

	Co–O	Co–Co	Co–Co	Co–Co
	Co(oct)–O Co(tetra)–O	Co(oct)–Co(oct)	Co(tetra)–Co(oct) Co(tetra)–Co(tetra)	Co(oct)–Co(oct)
r/nm	0.195	0.285	0.338	0.495
N	5.4	6.0	9.3	6.0

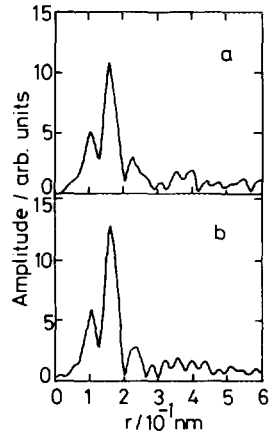

FIG. 5. The Fourier transforms of PTRF-EXAFS for sample [A]: (a) s- and (b) p-polarization.

The N^*'s for these arrangements can be calculated by the equations

$$N^*/3 = \cos^2\alpha \quad \text{(on-top sites)} \qquad [5]$$

$$= 2\cos^2\alpha\cos^2\beta + 2\sin^2\alpha\sin^2\beta\cos^2\phi \quad \text{(bridge sites)} \qquad [6]$$

$$= 3\cos^2\alpha\cos^2\beta + 1.5\sin^2\alpha\sin^2\beta \quad \text{(three-fold hollow sites).} \qquad [7]$$

The electric-field vector is characterized by the polar angle α from the surface normal and the azimuthal angle ϕ in the surface plane, and β is the bond angle from the surface normal (20). For the bridge sites $\cos^2\phi$ was integrated in every direction because of its equivalence. For the on-top position, the EXAFS oscillation parallel to the surface should not appear.

Assuming an ideal surface with O–O distance of 0.275 nm and using the Co–O bond length of 0.208 nm which was determined by the EXAFS analysis, we calculated the N^*'s in s- and p-polarized EXAFS and their ratio in each case; ∞ for on-top, 2.6 for bridge, and 1.4 for three-fold hollow (Table 2). The observed value, 1.2, is well reproduced only by a three-fold hollow site model. Furthermore, if Co atoms occupy the three sites heterogeneously, the observed value should be larger than 1.4. But this is not the case.

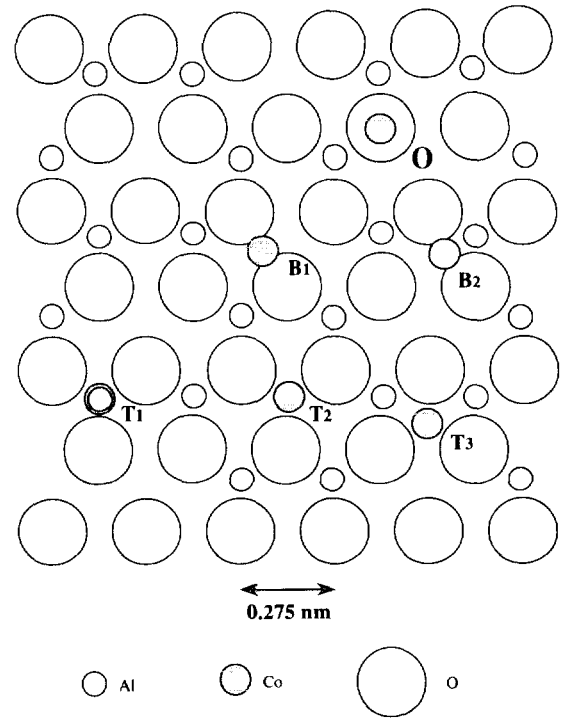

FIG. 6. Possible Co sites on α-Al_2O_3 (0001) surface: O, on-top site; B_1, B_2, bridge sites; T_1–T_3, threefold hollow sites.

The number of Co atoms was one-third the number of surface oxygen atoms as determined by XPS (Table 3). A known amount of $Co(NO_3)_2 \cdot 6H_2O$, 3.7×10^{14} Co atoms/cm^2, was deposited on α-quartz(0001). This sample was used as a reference for Co analysis. The XPS spectra were taken on a VG ESCA LAB5 (Al$K\alpha$, 10.5 keV, 20 mA). The binding energy of Co $2p_{3/2}$ level in the sample [A] and reference and the intensity ratio, $I(Co(2p_{3/2}))/I(O(1s))$, are shown in Table 3. The Co concentration of

TABLE 2

Experimental Results and Model Calculations of the Effective Coordination Number (N^*) for the Sample [A]

Polarization	Bond distance/nm	Effective coordination number (N^*)			
		Experimental	On top	Bridge	Three-fold
s	0.208	3.3[a]	0	1.3	2.6
p	0.208	3.9[a]	3	3.3	3.7
Ratio (p/s)		1.2	∞	2.6	1.4

[a] ± 0.7.

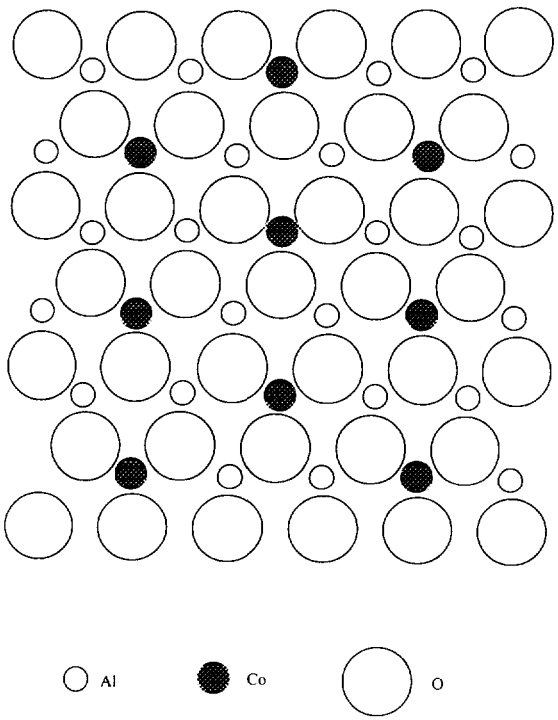

FIG. 7. Distribution of Co atoms in sample [A] by PTRF-EXAFS and XPS.

the sample [A] was calculated to be 6.7×10^{14} atoms/cm^2, which corresponds to one-third of the surface O atoms (1.7×10^{15} atoms/cm^2 assuming ideal surface structures of α-Al_2O_3 (0001)). The XPS result supports the conclusion that Co atoms exist on the threefold hollow sites of α-Al_2O_3 (T_1–T_3 in Fig. 6). The XPS binding energy for Co $2p_{3/2}$, 780.6 eV in Table 3, is similar to that for CoO (779.4–780.8 eV). Moreover, in *p*-polarized EXAFS, no Co–Al peak was observed. There are three kinds of threefold hollow sites on α-Al_2O_3 (0001) as shown in Fig. 6. Among them, only the T_2 site has no adjacent second-layer Al atom. The possibility of T_1 and T_3 for Co sites is excluded. The distribution of Co atoms on α-Al_2O_3 (0001) in the sample [A] is shown in Fig. 7. Such a selective adsorption may be due to a repulsive Coulomb interaction between Al atoms and Co atoms.

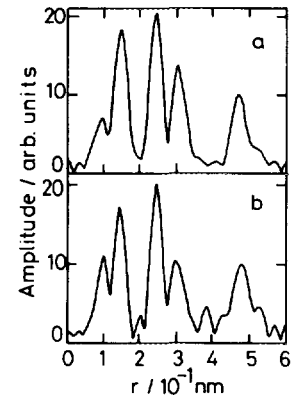

FIG. 8. The Fourier transforms of PTRF-EXAFS for sample [B]: (a) *s*- and (b) *p*-polarization.

In this monomer structure, Co atoms make bonds with three oxygen atoms of the Al_2O_3 lattice. The Co atoms have unsaturated coordination sites, but there exists no active oxygen atom. Thus the Co oxides on α-Al_2O_3 (0001) (sample [A]) did not show high activity for CO oxidation (Fig. 4).

3.2. Structure of Co Oxides on the α-Al_2O_3 (0001) Surface (Sample [B])

The 873 K-oxidation of sample [A] changed the surface structure from monomers (Fig. 5) to clusters (Fig. 8). The Fourier transforms in Fig. 8 resemble those in Fig. 3 for Co_3O_4, indicating that the spinel structure of Co oxides was formed by the high temperature oxidation. It was found that the intensities of the second (Co(oct)–Co(oct)) and third (Co(oct)–Co(tetra) and Co(tetra)–Co(tetra)) peaks are different with *s*- and *p*-polarization. The curve-fitting analysis for both the sets of polarized EXAFS data is shown in Table 4. The intensity of the second peak in *p*-polarization was 87% and the intensity of the third peak was 76%, respectively, compared to those in *s*-polarization. This means that Co-oxides grew to the spinel structure on α-Al_2O_3 (0001) asymmetrically. Moreover, the intensity of the fourth shell in both polarizations decreased to half of that for Co_3O_4 spinel. Based on the curve-fitting result, the half intensity of the fourth shell

TABLE 3

XPS Analysis for Surface Concentration of Co Atoms in the Sample [A]

Sample	Co $2p_{3/2}$/eV[a]	$I(Co(2p_{3/2}))/I(O(1s))$	Surface Co concentration[b]
Co/α-Al_2O_3 (0001) [A]	780.6	0.053	6.7×10^{14}
Reference	781.8	0.029	3.7×10^{14}

[a] referred to 285.0 eV for C(1*s*).
[b] Atoms/cm^2.

TABLE 4

Polarized Total-Reflection Fluorescene EXAFS Analyses for Sample (B)[a]

	Co–O			Co–Co			Co–Co			Co–Co		
Polarization	N^*	r/nm	σ/nm	N^*	r/nm	σ/nm	N^*	r/nm	σ/nm	N^*	r/nm	σ/nm
s	4.2	0.194	0.0036	6.9	0.286	0.0074	9.3	0.342	0.0077	3.1	0.496	0.0048
p	5.2	0.192	0.0071	6.0	0.285	0.0074	7.1	0.340	0.0077	2.7	0.497	0.0041

[a] For Co–O, N^*: ± 0.6, r: ± 0.002 nm; for Co–Co, N^*: ± 0.1–0.3, r: ± 0.001–0.002 nm.

means that the spinel size on α-Al_2O_3 (0001) is about 0.9 nm.

The ratios of the N^*'s for both polarizations in the second and third peaks were calculated for the cases where Co_3O_4 spinel (001), (110), and (111) planes grew parallel to the substrate (0001) plane in Fig. 9. In each case, two kinds of layers are placed alternately. For the (001) plane, one layer consists of oxygen atoms and octahedral Co atoms (001-A of Fig. 9) and the other layer consists of tetrahedral Co atoms (001-B). In case of the (110) plane, one layer consists of oxygen atoms and tetrahedral and octahedral Co atoms (110-A), and the other layer consists of octahedral Co atoms and oxygen atoms (110-B). For the (111) plane one layer is composed of oxygen atoms and octahedral Co atoms (111-A), and the other layer is composed of tetrahedral Co atoms (111-B). The expected N^* ratios are shown for different layer numbers. It was found that the (001-A) model with seven layers well reproduced the observed data. No other models fit the observed ratio. The spinel structure of Co oxides with seven layers on α-Al_2O_3 (0001) is illustrated in Fig. 10.

The spinel (001) plane is a close-packed plane and one of the stable surfaces. The preferential growth of the (001) plane parallel to α-Al_2O_3 (0001) surface may be due to the repulsion between the surface oxygen atoms of α-Al_2O_3 (0001) and the interface oxygen atoms of Co_3O_4 (001) being less than the repulsion for the cases of the (110) or (111) planes. However, the fit of the two planes is still not geometrically good as shown in Fig. 11. Therefore, a long-range two-dimensional layer of the (001) plane cannot be formed on α-Al_2O_3 (0001).

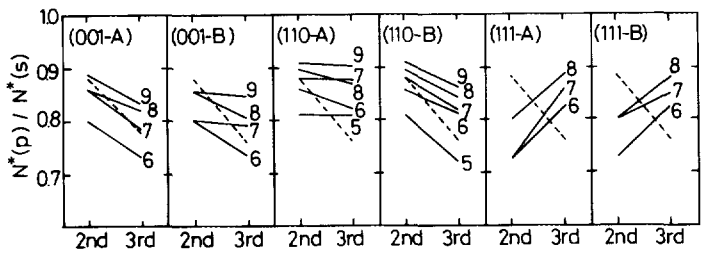

FIG. 9. Simulation of the ratio of the effective coordination numbers (p-/s-polarization) for each plane with different layers.

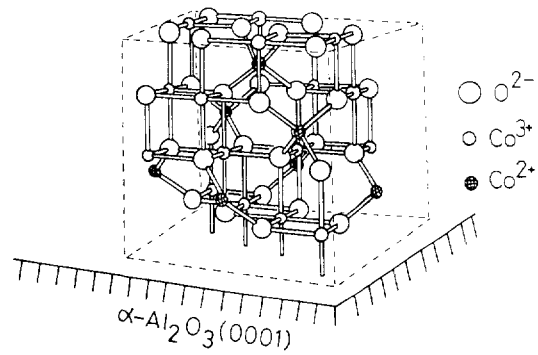

FIG. 10. Co_3O_4 spinel structures in 0.9 nm dimension with the (001) plane parallel to α-Al_2O_3 (0001).

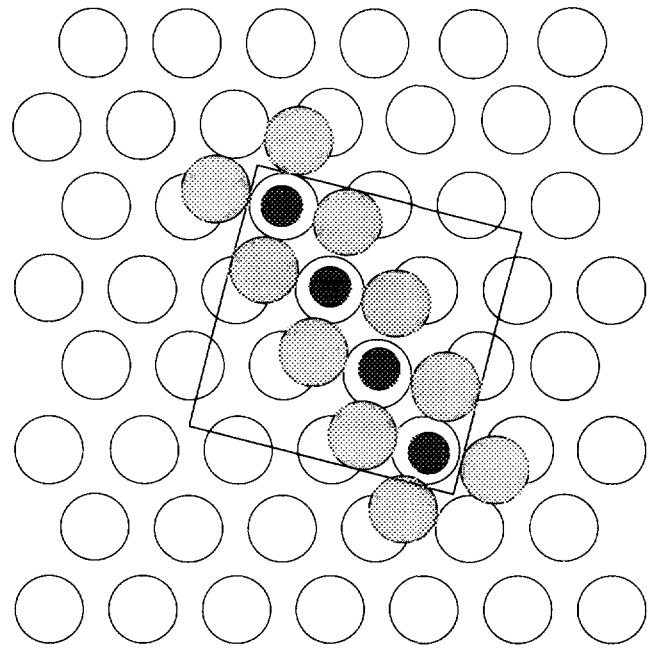

FIG. 11. An interface model of the Co_3O_4 (001) plane on the α-Al_2O_3 (0001) surface. Filled circles: Co atoms; shaded circles: O atoms of Co_3O_4 (001) plane; open circles: surface O atoms of α-Al_2O_3 (0001). The second layer Al atoms are not shown.

The small Co_3O_4 spinel structures of seven layers with the (001) plane parallel to the α-Al_2O_3 (0001) surface and with 0.9 nm size have coordinatively unsaturated oxygen atoms bridging two Co^{3+} ions in Fig. 10. It is to be noted that the sample [B] derived from $Co_2(CO)_8$ and α-Al_2O_3 (0001) exhibited a remarkably high activity for CO oxidation at low temperatures as compared with Pt or Pd catalyst (Fig. 4).

4. CONCLUSIONS

(1) Highly active cobalt oxides on α-Al_2O_3 (0001) were prepared and the active structures were determined by PTRF-EXAFS.

(2) In the sample [A] prepared with $Co_2(CO)_8$ vapor and α-Al_2O_3 (0001) and treated with O_2 at 300 K, cobalt atoms exist as monomers on the threefold hollow sites of α-Al_2O_3 (0001).

(3) After oxidation of the sample [A] with O_2 at 873 K (sample [B]), small spinel particles of seven-layer cobalt oxides grew with the (001) plane parallel to α-Al_2O_3 (0001).

ACKNOWLEDGMENT

We thank Professor Nomura (KEK-PF) for helpful discussion and for suggestions on PTRF-EXAFS.

REFERENCES

1. Iwasawa, Y., *Adv. Catal.* **35,** 187 (1987).
2. Iwasawa, Y., "Tailored Metal Catalysis." Reidel, Dortrecht, 1986.
3. Bart, J. C. J., and Vlaic, G., *Adv. Catal.* **35,** 1 (1987).
4. Stern, E. A., *Phys. Rev. B* **10,** 3027 (1974).
5. Heald, S. M., Keller, E., and Stern, E. A., *Phys. Lett. A* **103,** 155 (1984).
6. Hoffman, P., Lieser, E., Hein, M., and Flakowski, M., *Spectrochem. Acta Part B* **44,** 433 (1986).
7. Share, L. R., Heinman, W. R., and Elder, R. C., *Chem. Rev.* **90,** 705 (1990).
8. Frahm, R., Barbee, T. W., Jr., and Warburtron, W., *Phys. Rev. B* **44,** 2823 (1991).
9. Shirai, M., Asakura, K., and Iwasawa, Y., *Chem. Lett.*, 1037 (1992).
10. Shirai, M., Asakura, K., and Iwasawa, Y., *Shokubai* **34,** 416 (1992).
11. Shirai, M., Asakura, K., and Iwasawa, Y., *Catal. Lett.* **15,** 247 (1992).
12. Shirai, M., Asakura, K., and Iwasawa, Y., *Jpn. J. Appl. Phys.* **32,** 413 (1993).
13. Iwasawa, Y., Yamada, M., Sato, Y., and Kuroda, H., *J. Mol. Catal.* **23,** 95 (1984).
14. Yamada, M., and Iwasawa, Y., *Nippon Kagaku Kaishi,* 1042 (1984).
15. Asakura, K., Shido, T., and Iwasawa, Y., *Shokubai* **29,** 66 (1987).
16. Asakura, K., and Iwasawa, Y., *J. Phys. Chem.* **93,** 4213 (1989).
17. Sato, Y., and Iitaka, Y., *Res. Sci. Instrum.* **60,** 2390 (1989).
18. Teo, B. K., "EXAFS Spectroscopy: Basic Principles and Data Analysis" Inorganic Chemistry Concepts, Vol. 9. Springer-Verlag, Berlin, 1986.
19. Wryckoff, R. W. G., "Crystal Structure," 2nd ed. Interscience, New York (1964).
20. Stöhr, J., Jaeger, R., and Brennan, S., *Surf. Sci.* **117,** 503 (1982).